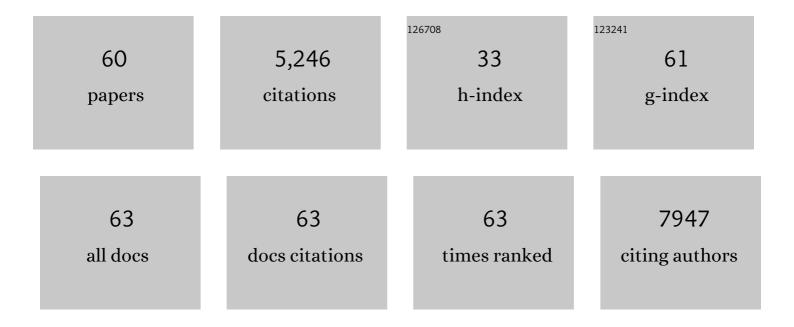
List of Publications by Year in descending order

Source: https://exaly.com/author-pdf/5649284/publications.pdf

Version: 2024-02-01



ΜλΟΙΙΙΝ ΥλΝΟ

#	Article	IF	CITATIONS
1	The coupling mechanism of mammalian mitochondrial complex I. Nature Structural and Molecular Biology, 2022, 29, 172-182.	3.6	45
2	A SYBR Gold-based Label-free in vitro Dicing Assay. Bio-protocol, 2022, 12, e4382.	0.2	1
3	AcrIF5 specifically targets DNA-bound CRISPR-Cas surveillance complex for inhibition. Nature Chemical Biology, 2022, 18, 670-677.	3.9	10
4	Structural basis for the catalytic activity of filamentous human serine beta-lactamase-like protein LACTB. Structure, 2022, 30, 685-696.e5.	1.6	8
5	Insights into the inhibition of type I-F CRISPR-Cas system by a multifunctional anti-CRISPR protein AcrIF24. Nature Communications, 2022, 13, 1931.	5.8	16
6	Discovery of small-molecule activators of nicotinamide phosphoribosyltransferase (NAMPT) and their preclinical neuroprotective activity. Cell Research, 2022, 32, 570-584.	5.7	27
7	Structure of intact human MCU supercomplex with the auxiliary MICU subunits. Protein and Cell, 2021, 12, 220-229.	4.8	34
8	The structural basis of function and regulation of neuronal cotransporters NKCC1 and KCC2. Communications Biology, 2021, 4, 226.	2.0	48
9	Structure of the full-length human Pannexin1 channel and insights into its role in pyroptosis. Cell Discovery, 2021, 7, 30.	3.1	14
10	Molecular insights into the human ABCB6 transporter. Cell Discovery, 2021, 7, 55.	3.1	18
11	Insights into the dual functions of AcrIF14 during the inhibition of type I-F CRISPR–Cas surveillance complex. Nucleic Acids Research, 2021, 49, 10178-10191.	6.5	9
12	Mechanism of siRNA production by a plant Dicer-RNA complex in dicing-competent conformation. Science, 2021, 374, 1152-1157.	6.0	58
13	Cryo-EM structures and transport mechanism of human P5B type ATPase ATP13A2. Cell Discovery, 2021, 7, 106.	3.1	16
14	Atomic structure of human TOM core complex. Cell Discovery, 2020, 6, 67.	3.1	67
15	Molecular insights into the human CLC-7/Ostm1 transporter. Science Advances, 2020, 6, eabb4747.	4.7	31
16	Distinct structural modulation of photosystem I and lipid environment stabilizes its tetrameric assembly. Nature Plants, 2020, 6, 314-320.	4.7	30
17	Research journey of respirasome. Protein and Cell, 2020, 11, 318-338.	4.8	22
18	Cryo-EM structure of the mammalian ATP synthase tetramer bound with inhibitory protein IF1. Science, 2019, 364, 1068-1075.	6.0	145

#	Article	IF	CITATIONS
19	Structure and mechanism of mitochondrial electron transport chain. Biomedical Journal, 2018, 41, 9-20.	1.4	133
20	UQCRFS1N assembles mitochondrial respiratory complex-III into an asymmetric 21-subunit dimer. Protein and Cell, 2018, 9, 586-591.	4.8	8
21	A binding-block ion selective mechanism revealed by a Na/K selective channel. Protein and Cell, 2018, 9, 629-639.	4.8	14
22	Structural basis of ubiquitin modification by the Legionella effector SdeA. Nature, 2018, 557, 674-678.	13.7	69
23	Structure of the intact 14-subunit human cytochrome c oxidase. Cell Research, 2018, 28, 1026-1034.	5.7	159
24	Cryo-EM structure of the ASIC1a–mambalgin-1 complex reveals that the peptide toxin mambalgin-1 inhibits acid-sensing ion channels through an unusual allosteric effect. Cell Discovery, 2018, 4, 27.	3.1	28
25	Temperature-dependent ESR and computational studies on antiferromagnetic electron transfer in the yeast NADH dehydrogenase Ndi1. Physical Chemistry Chemical Physics, 2017, 19, 4849-4854.	1.3	8
26	Structural insights into the coordination of plastid division by the ARC6–PDV2 complex. Nature Plants, 2017, 3, 17011.	4.7	29
27	Determining EGFR-TKI sensitivity of G719X and other uncommon EGFR mutations in non-small cell lung cancer: Perplexity and solution. Oncology Reports, 2017, 37, 1347-1358.	1.2	63
28	Target Elucidation by Cocrystal Structures of NADH-Ubiquinone Oxidoreductase of <i>Plasmodium falciparum</i> (<i>Pf</i> NDH2) with Small Molecule To Eliminate Drug-Resistant Malaria. Journal of Medicinal Chemistry, 2017, 60, 1994-2005.	2.9	51
29	Architecture of Human Mitochondrial Respiratory Megacomplex I2III2IV2. Cell, 2017, 170, 1247-1257.e12.	13.5	362
30	Cryo-EM structures of the mammalian endo-lysosomal TRPML1 channel elucidate the combined regulation mechanism. Protein and Cell, 2017, 8, 834-847.	4.8	39
31	Identification of Intracellular β-Barrel Residues Involved in Ion Selectivity in the Mechanosensitive Channel of Thermoanaerobacter tengcongensis. Frontiers in Physiology, 2017, 8, 832.	1.3	2
32	Structural basis of the interaction between the meningitis pathogen <i>Streptococcus suis</i> adhesin Fhb and its human receptor. FEBS Letters, 2016, 590, 1384-1392.	1.3	11
33	Structure of Mammalian Respiratory Supercomplex I 1 III 2 IV 1. Cell, 2016, 167, 1598-1609.e10.	13.5	311
34	TMCO1 Is an ER Ca 2+ Load-Activated Ca 2+ Channel. Cell, 2016, 165, 1454-1466.	13.5	112
35	The architecture of the mammalian respirasome. Nature, 2016, 537, 639-643.	13.7	311
36	Amazing structure of respirasome: unveiling the secrets of cell respiration. Protein and Cell, 2016, 7, 854-865.	4.8	38

#	Article	IF	CITATIONS
37	Crystal structures of Bbp from Staphylococcus aureus reveal the ligand binding mechanism with Fibrinogen α. Protein and Cell, 2015, 6, 757-766.	4.8	16
38	Expression, purification, crystallization and structure determination of the N terminal domain of Fhb, a factor H binding protein from Streptococcus suis. Biochemical and Biophysical Research Communications, 2015, 466, 413-417.	1.0	4
39	Structure of the eukaryotic MCM complex at 3.8 Ã Nature, 2015, 524, 186-191.	13.7	207
40	Structural basis for substrate specificity of an amino acid ABC transporter. Proceedings of the National Academy of Sciences of the United States of America, 2015, 112, 5243-5248.	3.3	49
41	Architecture of the mammalian mechanosensitive Piezo1 channel. Nature, 2015, 527, 64-69.	13.7	363
42	Functional and Structural Characterization of the Antiphagocytic Properties of a Novel Transglutaminase from Streptococcus suis. Journal of Biological Chemistry, 2015, 290, 19081-19092.	1.6	22
43	Structural insights into the TRIM family of ubiquitin E3 ligases. Cell Research, 2014, 24, 762-765.	5.7	118
44	Planar substrate-binding site dictates the specificity of ECF-type nickel/cobalt transporters. Cell Research, 2014, 24, 267-277.	5.7	39
45	Structural basis for hijacking CBF-β and CUL5 E3 ligase complex by HIV-1 Vif. Nature, 2014, 505, 229-233.	13.7	185
46	Hat2p recognizes the histone H3 tail to specify the acetylation of the newly synthesized H3/H4 heterodimer by the Hat1p/Hat2p complex. Genes and Development, 2014, 28, 1217-1227.	2.7	33
47	Structures of SdrD from Staphylococcus aureus reveal the molecular mechanism of how the cell surface receptors recognize their ligands. Protein and Cell, 2013, 4, 277-285.	4.8	30
48	Perilipin1 promotes unilocular lipid droplet formation through the activation of Fsp27 in adipocytes. Nature Communications, 2013, 4, 1594.	5.8	200
49	Crystal Structures Reveal the Multi-Ligand Binding Mechanism of Staphylococcus aureus ClfB. PLoS Pathogens, 2012, 8, e1002751.	2.1	51
50	Structural insight into the type-II mitochondrial NADH dehydrogenases. Nature, 2012, 491, 478-482.	13.7	105
51	When MAGE meets RING: insights into biological functions of MAGE proteins. Protein and Cell, 2011, 2, 7-12.	4.8	46
52	MAGE-RING Protein Complexes Comprise a Family of E3 Ubiquitin Ligases. Molecular Cell, 2010, 39, 963-974.	4.5	388
53	Insights into Mad2 Regulation in the Spindle Checkpoint Revealed by the Crystal Structure of the Symmetric Mad2 Dimer. PLoS Biology, 2008, 6, e50.	2.6	86
54	p31comet Blocks Mad2 Activation through Structural Mimicry. Cell, 2007, 131, 744-755.	13.5	172

#	Article	IF	CITATIONS
55	Mechanistic Analysis of a Suicide Inactivator of Histone Demethylase LSD1â€. Biochemistry, 2007, 46, 6892-6902.	1.2	87
56	Structural Basis for the Inhibition of the LSD1 Histone Demethylase by the Antidepressant trans-2-Phenylcyclopropylamine,. Biochemistry, 2007, 46, 8058-8065.	1.2	213
57	Structural basis of histone demethylation by LSD1 revealed by suicide inactivation. Nature Structural and Molecular Biology, 2007, 14, 535-539.	3.6	170
58	Structural Basis for CoREST-Dependent Demethylation of Nucleosomes by the Human LSD1 Histone Demethylase. Molecular Cell, 2006, 23, 377-387.	4.5	306
59	Crystallization and preliminary crystallographic analysis of RSB-66, a novel round spermatid-specific protein. Acta Crystallographica Section D: Biological Crystallography, 2003, 59, 1853-1855.	2.5	4
60	Crystallization and preliminary crystallographic analysis of the extracellular fragment of FcαRI/CD89. Acta Crystallographica Section D: Biological Crystallography, 2003, 59, 2251-2253.	2.5	2